Oxygenated Fluorocarbons Adsorbed at Metal Surfaces: Chemisorption Bond Strengths and Decomposition

M. M. Walczak, P. K. Leavitt, and P. A. Thiel*†

Contribution from the Department of Chemistry and Ames Laboratory, Iowa State University, Ames, Iowa 50011. *Received December 24, 1986*

Abstract: We report studies of the adsorption bond strengths and decomposition of perfluorodiethyl ether and hexafluoroacetone on clean and oxygen-dosed Ru(001). Perfluorodiethyl ether bonds weakly to Ru(001) (39 kJ/mol) without decomposing. This binding energy is typical for a metal-adsorbate interaction in which the adsorbate donates electrons to the metal from the oxygen lone pair. Hexafluoroacetone bonds to the surface in both a weakly bonded configuration (38 kJ/mol) and a strongly bonded configuration (66-87 kJ/mol), and there is some decomposition. We compare the chemistry of these oxygenated *fluoro*carbons to analagous oxygenated *hydro*carbons. We propose that the net effect of fluorination is to weaken those chemisorption bonds which rely upon electron donation from the oxygen lone pairs *to* the metal but to strengthen the chemisorption bonds which rely primarily upon electron donation *from* the metal into antibonding C-O orbitals. Both phenomena can be explained by electronic effects resulting from fluorination.

I. Introduction

Adhesion and thermal stability of common lubricants, such as fluorinated polymeric ethers, at surfaces are not understood on a molecular scale. Important questions remain to be addressed at a fundamental level: How strongly is the molecule bonded to the surface? Which functional groups of the molecule bond? Does the molecule decompose? What are the decomposition products, and how do they interact with the surface? We have studied the adsorption and decompositon of simple oxygenated fluorocarbons at a metal surface, Ru(001), as part of a larger effort to understand the answers to these questions. We have chosen oxygenated molecules for which the surface chemistry of the nonfluorinated analogues is already well understood in order to determine the way in which substitution of fluorine for hydrogen changes adsorption bond strengths and decomposition pathways.

It is well-established that simple, oxygen-containing organic molecules form bonds to transition-metal centers (including surfaces) via the oxygen-containing functional group. However, the mechanism of the interaction depends largely on whether the C-O bond is saturated or unsaturated. In molecules which contain saturated C-O bonds, such as ethers and alcohols (or, by analogy, water), a weak bond to the surface is formed by electron donation from an oxygen lone pair to the metal.[1-4] Such an interaction typically contributes 40 kJ/mol to the chemisorption bond.[2-4] Fluorination may be expected to weaken the metal-oxygen bond of a molecule such as an ether by inductively depleting electron density at the oxygen lone pairs.

Molecules which contain unsaturated carbon-oxygen bonds, e.g., ketones and aldehydes, exhibit two types of metal bonds, η^1 and η^2. The first involves electron donation from oxygen lone pairs (sp^2 orbitals) to the metal, similar to the case for saturated carbon-oxygen groups. In this configuration, the molecule is tilted with an M-O-C angle of about 150°.[5] The bond to the surface is weak and comparable in magnitude to those formed by the ethers: 34 ± 3 kJ/mol for η^1-methanal (hereafter referred to as formaldehyde) on Ru(001),[6] 47-52 kJ/mol for η^1-propanone (hereafter referred to as acetone) on Ru(001) (ref 7 and present work), and 49 kJ/mol for η^1-acetone on Pt(111).[8,9] Fluorination is expected to weaken the η^1 bond, and indeed, Avery reports a chemisorption bond of 35 kJ/mol for η^1-1,1,1,3,3,3-hexafluoropropanone (hereafter referred to as hexafluoroacetone) on Pt(111),[10] lower by 14 kJ/mol than that for the nonfluorinated molecule. These values are summarized in Table I.

The second possible configuration is one in which the molecule bonds with the C=O bond more nearly parallel to the metal surface, or with C and O atoms nearly equidistant from a metal center. This can be understood through the Chatt-Dewar-Duncansen model of hydrocarbon bonding, in which an unsaturated hydrocarbon donates electron density into vacant metal orbitals while the metal back-bonds into geometrically and energetically accessible antibonding orbitals. Overlap between the metal orbitals and the carbon group's low-lying, vacant π^* orbital is maximized by an η^2-geometry. In short, the observation of η^2-carbonyl means that back-bonding into π^* orbitals is a major component of the metal-carbonyl bond. Consequently, C=O vibrational stretching frequencies are lower and C=O equilibrium bond lengths are longer for η^2-carbonyl than for η^1-carbonyl (e.g., ref 6-13), indicative of a weaker C=O bond in the former case.

A molecule such as an ether does not have empty low-lying orbitals that can accept back-donation from the metal, so the η^2-form is not observed for ethers. In molecules that contain carbonyl groups, both η^1- and η^2-bonds can form. The η^2-bond is favored over η^1 by electropositive metal centers and/or electron-withdrawing groups adjacent to the carbonyl, such as fluorine.[6-13] These two factors presumably favor η^2-bonds due to the lowering of the carbonyl π^* orbital acceptor energy levels on fluorination,[14] providing a better match to the energy levels of the metal donor orbitals. This picture is supported by the work of Deffeyes et al.,[15,16] who have studied adsorption of propene and 3,3,3-trifluoropropene on oxygen-dosed Mo(100). They find that the fluorinated molecule is more strongly bound by about 11 kJ/mol, which they attribute to enhancement of back-donation

† National Science Foundation Presidential Young Investigator (1984-1989), Alfred P. Sloan Foundation Fellow (1984-1986), and Camille and Henry Dreyfus Foundation Teacher-Scholar (1986-1990).

(1) Lüth, H.; Rubloff, G. W.; Grobman, W. D. *Surf. Sci.* **1977**, 63, 325.
(2) Sexton, B. A.; Hughes, A. E. *Surf. Sci.* **1984**, *140*, 227.
(3) Rendulič, K. D.; Sexton, B. A. *J. Catal.* **1982**, *78*, 126.
(4) Thiel, P. A.; Madey, T. E. *Surf. Sci. Rep.*, in press.
(5) Gould, R. O.; Sime, W. J.; Stephenson, T. A. *J. Chem. Soc., Dalton Trans.* **1978**, *1*, 76.
(6) Anton, A. B.; Parmeter, J. E.; Weinberg, W. H. *J. Am. Chem. Soc.* **1986**, *108*, 1823.
(7) Anton, A. B.; Avery, N. R.; Toby, B. H.; Weinberg, W. H. *J. Am. Chem. Soc.* **1986**, *108*, 684.
(8) Avery, N. R. *Surf. Sci.* **1983**, *125*, 771.
(9) Avery, N. R.; Weinberg, W. H.; Anton, A. B.; Toby, B. H. *Phys. Rev. Lett.* **1983**, *51*, 682.
(10) Avery, N. R. *Langmuir* **1985**, *1*, 162.
(11) Wood, C. D.; Schrock, R. R. *J. Am. Chem. Soc* **1979**, *101*, 5421.
(12) Countryman, R.; Penfold, B. R. *J. Cryst. Mol. Struct.* **1972**, *2*, 281.
(13) Tsou, T. T.; Huffman, J. C.; Kochi, J. K. *Inorg. Chem.* **1979**, *18*, 2311.
(14) Jorgensen, W. L.; Salem, L. *The Organic Chemist' Book of Orbitals*; Academic: New York, 1973. Comparison of the energy of the $2B_2$ orbital of formaldehyde and the 3A″ orbital of formyl fluoride.
(15) Deffeyes, J. E.; Horlacher Smith, A.; Stair, P. C. *Surf. Sci.* **1985**, *163*, 79.
(16) Deffeyes, J. E.; Horlacher Smith, A.; Stair, P. C. *Appl. Surf. Sci.*, in preparation.

0002-7863/87/1509-5621$01.50/0

Table I. Desorption Characteristics of η^1 and η^2 Carbonyls on Metal Surfaces

molecule	substrate	coordination	T_p, K	E_d, kJ/mol	thermal decomp	ref
$(CH_3)_2CO$	Pt(111)	η^1(majority)	185	49[a]	none	8, 9
$(CF_3)_2CO$	Pt(111)	η^1(majority)	135	35[a]	none	10
$(CH_3)_2CO$	Ru(001)	η^1(minority)	200–400	42–62[a]	none	7
			195–210	48–52[b]	none	present work
$(CH_3)_2CO$	O/Ru(001)	η^1(majority)	200–450	42–79[a]	none	7
$(CF_3)_2CO$	Ru(001)	(α_3)	157	38[b]		present work
H_2CO	Ru(001)	η^1(minority)	130–155	31–37[a]	none	6
H_2CO	O/Ru(001)	η^1(majority)	130–155	31–37[a]	none	6
$(CH_3)_2CO$	Pt(111)	η^2(minority)	220–240	58–64[b]	extensive	8
$(CH_3)_2CO$	Ru(001)	η^2(majority)			extensive	7
$(CH_3)_2CO$	O/Ru(001)	η^2(minority)			extensive	7
$(CF_3)_2CO$	Ru(001)	(α_1)	346	87[b]		present work
H_2CO	Ru(001)	η^2(majority)	275	67[a]	extensive	6

[a] Taken from literature reference cited. [b] Calculated from T_p according to ref 17, assuming $\nu = 10^{13}$ s^{-1} and simple first-order kinetics.

from the metal into the π^* C=C bond of the undissociated molecule.[15,16]

On metal surfaces, η^2-carbonyls tend to decompose via C–H or C–C bond cleavage rather than desorb,[6-9] but there is one report that η^2-acetone desorbs intact from Pt(111) at 220–240 K,[8] which corresponds to a chemisorption bond of 61 ± 3 kJ/mol.[17] This is 12 kJ/mol higher than for η^1-acetone on the same surface, consistent with the idea that η^2-coordination provides a stronger bond with the metal than η^1. (See Table I.)

In addition to the metal–oxygen bond, there appears to be a weak attractive interaction between hydrocarbon groups and the surface. Sexton and co-workers have shown that the desorption energy of chemisorbed ethers, alcohols, and alkanes on Cu and Pt surfaces is proportional to the number of carbon atoms in the aliphatic portion of the molecule.[2,3] As the hydrocarbon chain length increases, desorption energy increases (and is reflected by an increase in desorption peak temperature) because the metal can interact favorably with more $-CH_2-$ groups. Sexton and Hughes have shown that this interaction contributes 5 to 6.5 kJ/mol per CH_2 group for ethers adsorbed on Pt(111).[2] A similar phenomenon has been observed for saturated cyclic hydrocarbons adsorbed on Ru(001), where desorption energy increases linearly with the number of CH_2 groups.[18] Hoffmann and Upton report that this is not attributable to hydrogen bonding between the hydrocarbon and the metal but rather due to a more complex interaction with several opposing components.[19] The *net* interaction is probably less favorable for a CF_2 group than for a CH_2 group, partly because the C–F bond is longer than the C–H bond (1.32 Å in C_2F_6 vs. 1.10 Å in C_2H_6[20]) and partly because fluorine is more electron-rich than hydrogen.[21] The carbon is held farther away from the surface by the first factor, and fluorine–metal repulsion is important due to the second factor.

In the case of an η^2-carbonyl there is an additional factor to consider: on an atomically flat metal surface, the η^2-geometry requires either that the aliphatic portions of the molecule approach the metal surface closely or else that there is some rehybridization about the acyl carbon. The latter is believed to take place in η^2-acetone on Ru(001).[7] As described above, we expect that it is more difficult for a bulky fluorinated aliphatic group to approach a metal surface than for a hydrogenated group. In turn, this may require that either an η^2-geometry adopts a higher degree of rehybridization or else it is entirely prevented from forming, in a fluorinated molecule. Indeed, Avery observes that η^1-coordination predominates for hexafluoroacetone on Pt(111),[10] even though fluorination is known to favor η^2-coordination in inorganic complexes of hexafluoroacetone.[12] This may represent the effect of steric hindrance.

In summary, a fluorinated *ether* is expected to bind more weakly to a transition-metal surface than its nonfluorinated analogue, because fluorination weakens both the oxygen–metal interaction and the carbon–metal interaction. A fluorinated *carbonyl* may bind more or less strongly to a metal surface, depending upon which of two coordinations is adopted: Repulsive interactions between the bulky fluorocarbon chain(s) and the metal may force the molecule into the η^1-form, even though inductive electron withdrawal from the carbonyl group favors η^2-coordination. In the former case, an η^1-bond is expected to be weaker for the fluorocarbon than for the hydrocarbon, but an η^2-bond (if formed) should be stronger when the same comparison is made, and it may lead to decoposition of the molecule.[7-9] The purpose of the preent work is to test these hypotheses.

We find that the chemisorption bond of 1,1′-oxybis(perfluoroethane) (hereafter referred to as perfluorodiethyl ether) on Ru(001) is relatively weak, as expected (39 kJ/mol), and less than 0.002 monolayer decomposes. By contrast, about 0.005 monolayer of hexafluoroacetone decomposes. The remaining chemisorbed hexafluoroacetone molecules desorb from several states. One with relatively high binding energy, 87 kJ/mol, is suppressed by coadsorbed oxygen. These findings suggest an η^2-coordination within the first layer, the first observation of η^2-coordination for a fluorinated carbonyl on a metal surface.

II. Experimental Procedures

The experiments are performed in two stainless steel UHV chambers with base pressures of 4×10^{-10} and 1×10^{-10} Torr. Both chambers are equipped with a mass spectrometer, an ion gun, and a gas inlet manifold. One chamber is also equipped with an Auger spectrometer. The two Ru(001) samples, about 1 cm^2 in area, are grown at the Ames Laboratory Materials Preparation Center. They are oriented and polished to within ±1 deg of the (001) face on both sides. The initial crystal cleaning procedure under vacuum includes successive heating, ion bombardment, and oxidation cycling.[22] The sample cleanliness is checked by measuring TDS of CO following oxygen exposure and by Auger electron spectroscopy (AES). Two 0.020-in. Ta wires are spotwelded to the edges of the sample. The Ta wires are attached to a liquid-nitrogen-coolable cold-finger and are used to resistively heat the sample.[23] The crystal temperature is measured with a W-5% Re vs. W-26% Re thermocouple spotwelded to the edge of the sample. The sample can be cooled from 1600 to 90 K in 5 min.

The oxygenated hydrocarbons used in this study, acetone and 1,1′-oxybis(ethane) (hereafter referred to as diethyl ether), are reagent grade. The acetone, from Malinckrodt, is specified as 99.88% pure. The anhydrous diethyl ether, from Fischer, is specified as 99.9% pure. These compounds are further purified by repeated freeze–pump–thaw cycles on the gas-handling manifold.

The oxygenated fluorocarbons are purchased from Strem Chemical Co. The vendor specifies that the ether is 98% pure and the hexa-

(17) Redhead, P. A. *Vacuum* **1962**, *12*, 203. Rather than solve for E_d using eq 6 of this reference, we solve the exact equation iteratively: $E_d/kT_p = \ln(\nu T_p/\beta) - \ln(E_d/kT_p)$. Note that the last term in this equation is approximated by Redhead as $\ln(\ln(\nu T_p/\beta))$, with a value of *3.64*. However, under the assumptions described by him, we calculate a value between 3.23 and 3.60, with a mean of *3.44*. A slight error is incurred by using eq 6 from Redhead directly.

(18) Madey, T. E.; Yates, J. T., Jr. *Surf. Sci.* **1978**, *76*, 397.

(19) Hoffmann, F. M.; Upton, T. H. *J. Phys. Chem.* **1984**, *88*, 6209.

(20) Mitchell, A. D.; Cross, L. C., Ed. *Tables of Interatomic Distances and Configurations in Molecules and Ions*; Burlington House: London, 1958.

(21) Chambers, R. D. *Fluorine in Organic Chemistry*; John Wiley and Sons: New York, 1973.

(22) Williams, E. D.; Weinberg, W. H. *Surf. Sci.* **1979**, *82*, 93.

(23) Thiel, P. A.; Anderegg, J. W. *Rev. Sci. Instrum.* **1984**, *55*, 1669.

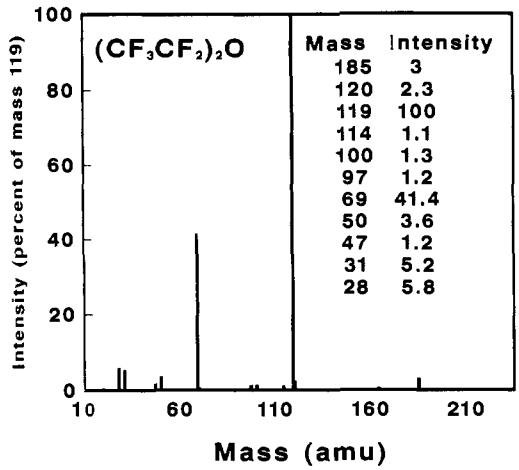

Figure 1. Mass spectrum of perfluorodiethyl ether. Electron energy 70 eV, accelerating voltage 8 kV.

fluoroacetone is at least 97% pure; these chemicals are used without further purification. A mass spectrum of each compound is obtained in situ and compared with a reference spectrum to check for decomposition in the stainless steel gas handling lines. The mass spectrum of perfluorodiethyl ether is not available in the literature. Therefore, it is measured independently on a Kratos MS50TC magnetic sector mass spctrometer and is shown in Figure 1. A hexafluoroacetone mass spectrum is also obtained on the Kratos system and compared with a published spectrum.[24] Upon comparison, the in situ spectra show no evidence for decomposition of any of the fluorocarbons in the gas lines.

Special safety precations are deemed necessary for handling these gases. Hexafluoroacetone, for instance, is "highly toxic by inhalation", with human tolerance reported to be 0.1 ppm in air.[25] (Specific toxicity data are not available for the fluorinated ether.) Within the gas manifold, most of the volume is evacuated by condensation into a liquid nitrogen trap, followed by evaporation of the trap contents into a hood; mechanical pump exhausts are also vented into the hood. The manifold and the venting system are tested for leaks by purging with H_2S. The human nose is sensitive to H_2S at levels of 0.03 ppm,[26] below the tolerance level of hexafluoroacetone. The absence of detectable odor during the test is therefore taken as evidence that fluorocarbons cannot escape at a rate sufficient to build up toxic levels. [There is no consequent evidence for sulfur contamination in the gas manifold following this procedure.]

The oxygenated fluorocarbons and hydrocarbons are introduced into the UHV chamber via a directed capillary array doser. The exposure units reported are Langmuir equivalents, arrived at by comparing exposures of CO through the doser with exposures from backfilling the chamber.

Between experiments the sample is cleaned by heating to 1300 K in 5×10^{-8} Torr of O_2 or by exposing the sample repeatedly to 5 L of O_2 and monitoring mass 28 as the sample is heated. It is then flashed under vacuum and held for 30 s at 1600 K to desorb the remaining oxygen until no oxygen Auger signal is seen. The sample is cooled to 90 K prior to each exposure to a fluorinated gas. Thermal desorption measurements are taken on an EAI Quad 150 mass spectrometer interfaced to a Commodore 64 computer or a PDP/11 computer. The spectrometer ionizer is in direct line-of-sight with the sample and about 10 cm removed. The computer allows (effectively) simultaneous detection of up to four masses (eight masses for the PDP/11) as a function of time and temperature. The sample temperature is controlled by a feedback circuit described previously by Herz et al.[27] The heating rate is held constant at 10 ± 1 K/s.

The extent of decomposition of the organic molecules is measured by monitoring CO desorption (28 amu) during each thermal desorption experiment. These areas are compared with those which result from saturation of the surface with CO and also from adsorption of background gases. The area that results from a saturation coverage of CO is known to represent an absolute coverage of 0.67 monolayers,[22] and this is used to calibrate all other desorption peak areas. For each experiment with the organic molecules, the area attributable to adsorption of CO from the background (≲0.002 monolayer) is subtracted from the total area of the CO desorption peak. We estimate that CO coverages below about 0.002 monolayer cannot be unambigously distinguished from background adsorption, i.e., this is about our lower limit of detection.

We adopt the following nomenclature: Desorption states which represent molecules measurably influenced by the metal surface (i.e., resolved from the bulklike multilayer) are labeled α, with a numerical subscript that corresponds to the sequence of population with increasing exposure. Desorption states which represent sublimation from bulklike multilayers are labeled γ. Peak temperatures in the text and figures are rounded to the nearest 5 K.

In some cases, the thermal desorption spectra of the fluorinated compounds are quite difficult to reproduce, particularly the high-temperature states. In order to distinguish questionable states from possible experimental artifacts, such as desorption from heating wires or desorption form the back side of the crystal, the following experiments are done: The Auger spectrum of the clean sample is recorded, showing no detectable oxygen. The Ru sample is then cooled to 90 K, exposed to the fluorined gas, and heated to a temperature which stops short of desorbing the state in question. The O/Ru Auger peak ratio is recorded. The entire sequence is then repeated, except that the thermal ramp is stopped after the questionable state has desorbed, and an Auger spectrum is again measured. In this way, we have shown that the α_1 state of hexafluoroacetone is indeed due to desorption from the Ru(001) surface. The difficult irreproducibility is most probably due to occasional inadequate cleaning procedures, specifically incomplete oxygen removal.

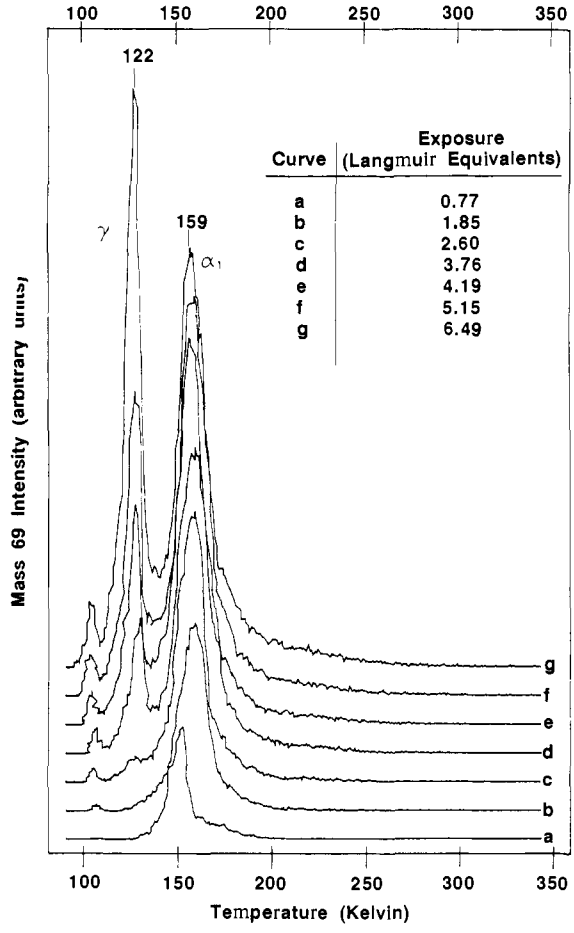

Figure 2. Thermal desorption spectra of perfluorodiethyl ether from Ru(001) following adsorption at 90 K.

III. Results

A. Perfluorodiethyl Ether. Themal desorption spectra following adsorption of $(CF_3CF_2)_2O$ at 90 K on Ru(001) are shown in Figure 2. The spectra are obtained by monitoring mass 69, CF_3^+, an intense molecular fragment, as a function of temperature. At low exposures a state at 160 K, which we denote α_1, grows in intensity as exposure increases and does not quite saturate before

(24) Heller, S. R.; Milne, G. W. A. *EPA/NIH Mass Spectral Data Base*; NSRDS-NBS63; U.S. Government Printing Office: Washington, D.C., 1978; Vol. 1.

(25) Hawley, G. G. *Condensed Chemical Dictionary*, 10th ed.; Van Norstrand Reinhold Co.: New York, 1981.

(26) Nielsen, J. M. *Material Safety Data Sheet Collection*; Genium Publishing Corp.: Schenectady, NY, 1979; Vol. 1.

(27) Herz, H.; Conrad, H.; Küppers, J. *J. Phys. E* **1979**, *12*, 369.

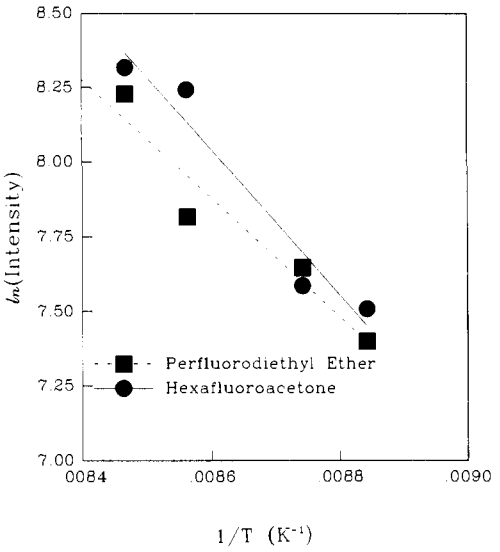

Figure 3. Clausius–Clapeyron analyses of the leading edges of the multilayer (γ) peaks for the oxygenated fluorocarbons.

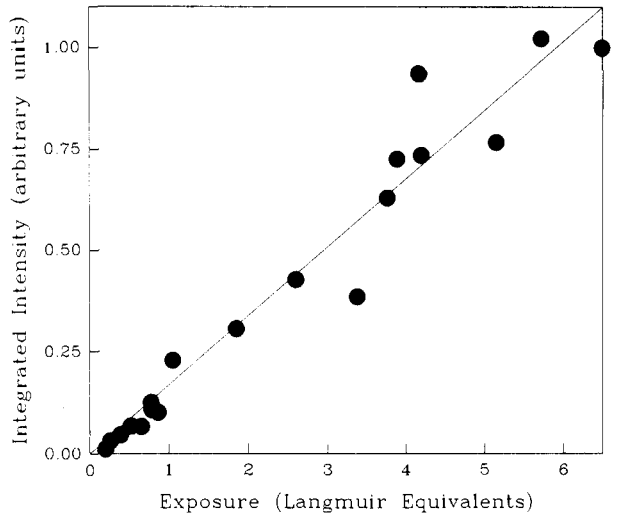

Figure 4. Integrated intensity of mass 69 desorption as a function of exposure of perfluorodiethyl ether.

a second state at 120 K, γ, begins to fill. The γ state does not saturate with increasing exposure.

The α_1 state displays the features characteristic of simple first-order desorption kinetics:[17] the peak temperature of 158 ± 4 K and the peak full-width at half-maximum (fwhm) of 19 ± 1 K are invariant with coverage, within the stated experimental error. We interpret the α_1 state to represent molecular desorption from a chemisorbed layer. Assuming a pre-exponential factor (ν) of 10^{13} s^{-1}, the peak temperature of 158 ± 4 K corresponds to a desorpiton barrier (E_d) of 39 ± 1 kJ/mol.[17]

The inability to saturate the γ state at high exposures indicates that this state is due to bulk sublimation. Zero-order anlaysis of the leading edge at high coverage, shown in Figure 3, yields a value for the heat of sublimation (E_s) of 16 ± 1 kJ/mol, where the uncertainty of ±1 kJ/mol represents the standard deviation in E_s obtained from three separate experiments.

The integrated desorption peak intensity is a linear function of exposure throughout the filling of the α_1 and γ states, as shown in Figure 4. Note that the line intersects the origin, which suggests that there is no decomposition. This is supported by the fact that the molecule adsorbs and desorbs reversibly, i.e., the desorption data can be reproduced repetitively without sample cleaning between successive experiments. In addition, during desorption there are no peaks associated with masses 38, 66, 78, 88, 100, and 119, which would be the masses expected for F_2, $F_2C{=}O$, $F_2C{=}C{=}O$, CF_4, $CF_2{=}CF_2$, or CF_3CF_2 (an intense molecular fragment of CF_3CF_3), respectively. A gradual rise occurs for all masses, however. Presumably, this is due to desorption from other parts of the manipulator as the sample temperature increases. [When heating to high temperatures (950 K), the assumption that the sample is adiabatic breaks down.] Calibration of the CO desorption peak, as described in section II, indicates that less than 0.002 monolayer of perfluorodiethyl ether decomposes.

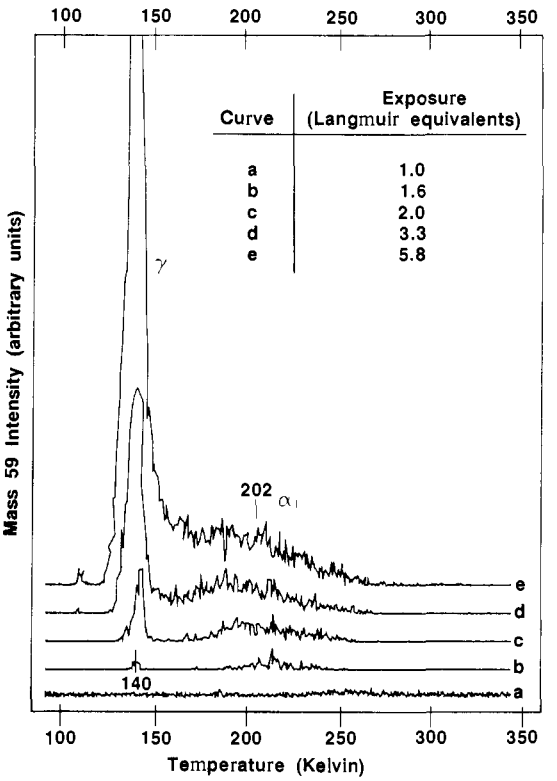

Figure 5. Thermal desorption spectra of diethyl ether from Ru(001) following adsorption at 90 K.

Table II. Decomposition of Oxygenated Fluorocarbons and Hydrocarbons on Ru(001)

	monolayers decomposing	
molecule	hydrogenated	fluorinated
diethyl ether	0.07	<0.002
acetone	0.17, 0.12[7]	0.005

For comparison, the thermal desorption spectra of diethyl ether from Ru(001) have also been measured and are shown in Figure 5. These spectra are obtained by monitoring $CH_3CH_2OCH_2^+$ at 59 amu, the largest molecular fragment. It can be seen that the spectra resemble those of perfluorodiethyl ether except that the analogous α_1 peak is much broader in the nonfluorinated case. The peak temperature of the α_1 state falls between 190 and 215 K, which corresponds to E_d = 47–53 kJ/mol.[17] Approximately 0.07 monolayer of diethyl ether decomposes. The amount of decomposition of the oxygenated fluoro- and hydrocarbons is summarized in Table II.

B. Hexafluoroacetone. Thermal desorption spectra obtained after adsorption of $(CF_3)_2CO$ on Ru(001) at 90 K are shown in Figure 6. The most intense molecular fragment, CF_3^+ at 69 amu,[24] is monitored as a function of temperature. At low exposure, a single peak at 345 K is populated (α_1), as shown in curves a and b. With increasing exposure two other features develop simultaneously at 265 and 155 K, which we designate α_2 and α_3, respectively. Finally, at high exposures, the α_1, α_2, and α_3 features saturate and a narrow peak at ca. 120 K emerges. The latter state (γ) cannot be saturated with increasing exposure.

The α_1, α_2, and α_3 states exhibit the same characteristics of first-order desorption as described for perfluorodiethyl ether. The peak characteristics, and the corresponding values of E_d (assuming $\nu = 10^{13}$ s^{-1}), are summarized in Table III for these three states.

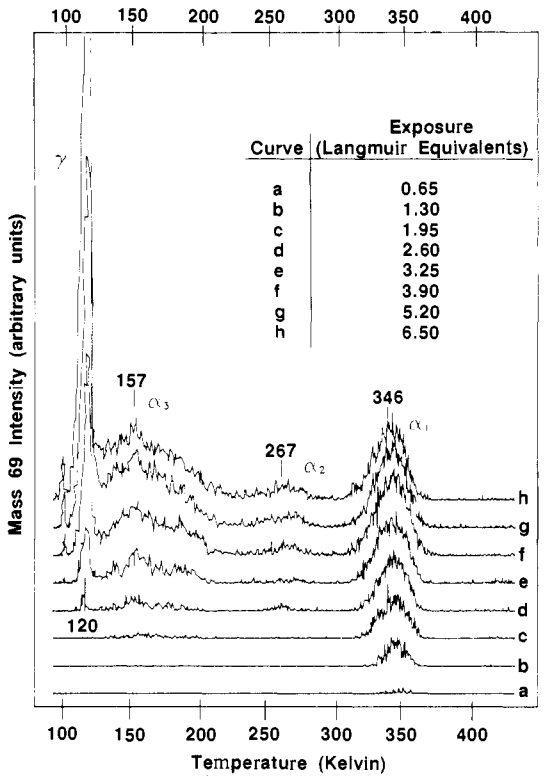

Figure 6. Thermal desorption spectra of hexafluoroacetone from Ru(001) following adsorption at 90 K.

Table III. Desorption Parameters for First-Order States of Hexafluoroacetone[a]

state	T_p,[b] K	fwhm,[b] K	E_d, kJ/mol
α_1	346 ± 1	22 ± 2	86.5 ± 0.3
α_2	267 ± 4	34 ± 7	66 ± 2
α_3	157 ± 1	61 ± 3	38.3 ± 0.4

[a] These values were calculated according to ref 17 assuming $\nu = 10^{13}$ s^{-1}, β = 10 K/s, and simple first-order kinetics. [b] The range of values indicates the variation over all coverages. For a simple first-order desorption peak, both T_p and the full-width at half-maximum (fwhm) remain constant (ref 17).

The integrated area under the α_3 peak, which is proportional to the number of molecules desorbing from that state, is 1.5 times larger than the area encompassed by the α_1 peak. Curves g and h of Figure 6 are used for this analysis since at these exposures both the α_1 and α_3 peaks are saturated. The α_1, α_2, and α_3 features clearly represent states that are strongly influenced by the metal surface.

The γ state is attributed to sublimation from the bulklike multilayer. A zero-order leading edge analysis, illustrated in Figure 3, indicates that the heat of sublimation at high coverage is 22 ± 2 kJ/mol. (The uncertainty given is the standard deviation in the heat of sublimation evaluated from three separate spectra.) This is in reasonable agreement with the known heat of sublimation of the bulk compound, which is 30 kJ/mol at the triple point, 147.70 K.[28] The integrated intensity of the total hexafluoroacetone spectrum is shown as a function of exposure in Figure 7. The changes in slope at exposures of ca. 1.5 and 2.5 Langmuir equivalents coincide with the onset of filling of the α_2 and a_3 states (curve c of Figure 6) and with the onset of population of the multilayer (curve d of Figure 6), respectively. No desorption of mass 69 is observed at exposures less than 0.3 Langmuir equivalents. This indicates that some decomposition occurs, supported by the observation that thermal desorption spectra are not reproducible unless the sample is carefully cleaned between each adsorption–desorption cycle. However, no peaks are present in the desorption traces of masses 38, 66, 78, 88, and 100 amu,

(28) Plausch, A. C.; Pace, E. L. *J. Chem. Phys.* **1967**, *47*, 44.

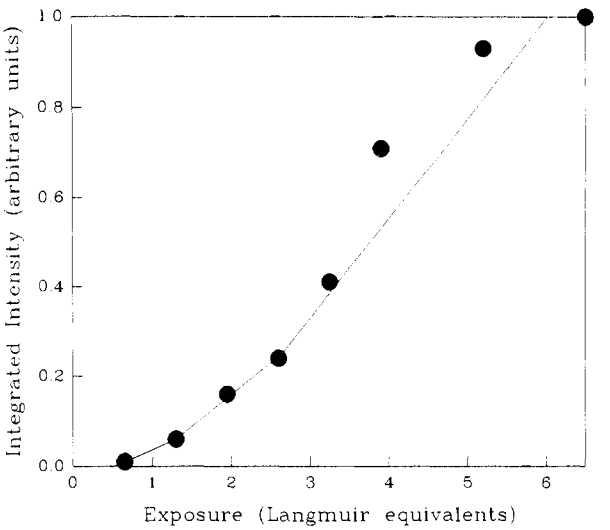

Figure 7. Integrated intensity of mass 69 desorption as a function of exposure of hexafluoroacetone.

corresponding to F_2, $F_2C{=}O$, $F_2C{=}C{=}O$, CF_4, and $CF_2{=}CF_2$. Only a slow and continuous intensity increase occurs for each of these masses, similar to the results described for perfluorodiethyl ether, at temperatures up to 1600 K. CO thermal desorption indicates that 0.005 monolayer of hexafluoroacetone decomposes (see Table II). Auger electron spectroscopy does not detect a fluorine residue following the TDS experiments, perhaps because the cross-section for electron-stimulated desorption is prohibitively high.

Adsorption of 0.5 L of oxygen at room temperature, with subsequent cooling to 90 K and exposure to ~5.2 Langmuir equivalents of hexafluoroacetone, results in suppression of the α_1 hexafluoroacetone state and desorption from a new state between the α_2 and α_3 states as shown in Figure 8. Coadsorption of 1 L of O_2 completely suppresses the α_1 state in favor of the new feature at ca. 215 K.

For comparison, thermal desorption spectra of acetone have also been measured and are shown in Figure 9. These spectra are obtained by monitoring CH_3CO^+, at 43 amu, the largest molecular fragment. The high-temperature state (α_1) desorbs between 195 and 210 K corresponding to E_d = 48–52 kJ/mol. Another notable feature in the desorption spectrum is the long, high-temperature tail on the α_1 peak. At high exposures a multilayer state at 150 K is populated. We find that 0.17 monolayers of acetone decompose on the saturated surface (Table II).

These data agree well with previous work by Anton et al.,[7] where acetone is reported to desorb in a broad peak between 200 and 400 K (E_d = 42–62 kJ/mol). Our desorption spectra are similar except that we resolve a peak at ca. 195–210 K (E_d = 47–52 kJ/mol). Anton et al. also report that 0.12 monolayer of acetone decomposes,[7] which is reasonably close to our value of 0.17. EELS results confirm the presence of both η_1- and η_2-acetone on Ru(001) in the chemisorbed layer.[7]

IV. Discussion

A. Perfluorodiethyl Ether. Perfluorodiethyl ether is a simple chemical model for commercially used polymeric perfluorinated lubricants, which are often ethers. Our present work shows that the chemisorption bond of the fluorinated ether on Ru(001) is rather weak, 39 kJ/mol, and is lower by 11 kJ/mol than the nonfluorinated ether. This is consistent with the ideas discussed in the Introduction, i.e., fluorination can only weaken one or both of the positive interactions of the molecule with the surface: electron donation from the oxygen lone pairs to the metal and attraction between CH_2 groups and the metal.

We find that less than 0.002 monolayer of perfluorodiethyl ether decomposes. In contrast, about 0.07 monolayer of diethyl ether decomposes on Ru(001) (see Table II) and 0.1 of a full layer of diethyl ether decomposes on Pt(111) to yield CO, H_2, and CH_x[2,3].

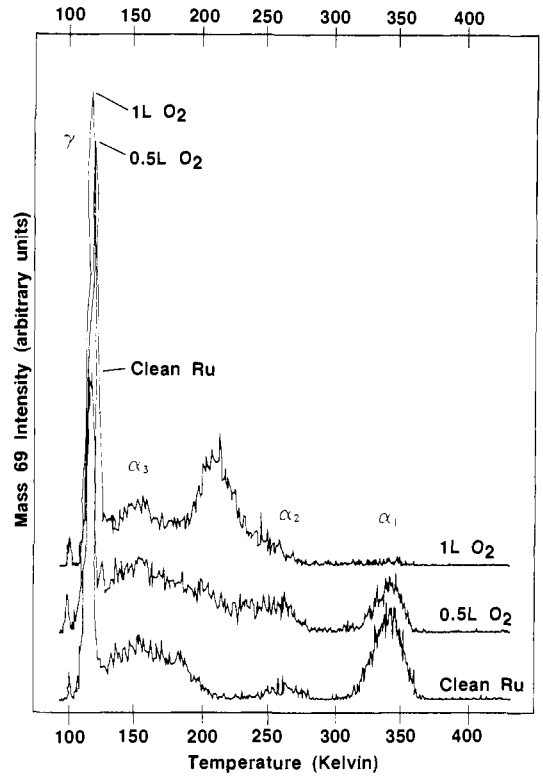

Figure 8. Effect of preadsorbed oxygen on thermal desorption states of hexafluoroacetone.

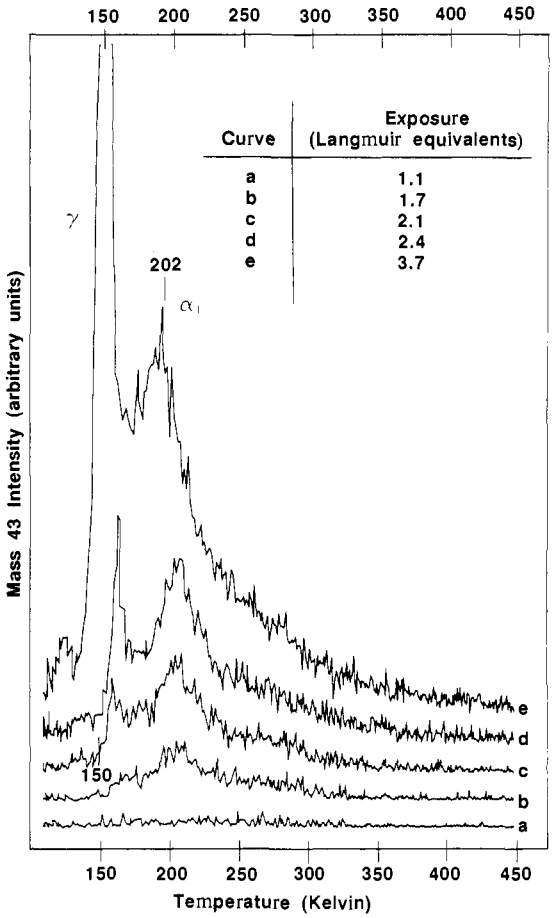

Figure 9. Thermal desorption spectra of acetone from Ru(001) following adsorption at 90 K.

A possible explanation is the difference between the C–H bond strength (410 kJ/mol in C_2H_6[29]) and the C–F bond strength (440 kJ/mol in C_5F_6[30]). This stabilization of the C–F bond may be important if decomposition of the molecule is limited by the rate of C–F or C–H bond breaking. A second possible explanation is that the hydrocarbon portion(s) of the molecule must approach the metal rather closely in order for the first internal molecular bond to break, whether that is the C–O, C–C, or C–H (C–F) bond. For the reasons introduced in section I, we believe it is not favorable for a saturated *fluoro*carbon segment to approach a metal surface as closely as the analogous saturated *hydro*carbon segment. This would effectively increase the energy barrier for metal-catalyzed decomposition of a fluorinated ether relative to that of the nonfluorinated molecule.

B. Hexafluoroacetone. Inspection of previously published data for ketones and aldehydes adsorbed on Pt(111),[8-10] Ru(001),[6,7,9] and oxygen predosed Ru(001),[6,7] summarized in Table 1, shows that the following generalizations are true:

(1) When a majority of molecules are bonded as η^1, the extent of decomposition is small or undetectable. Significant decomposition is associated with η^2-coordination.

(2) The chemisorption bond strengths of η^1-carbonyls are generally below 50 kJ/mol ($T_p < 200$ K), whereas the bond strengths of η^2-carbonyls are generally 60–70 kJ/mol and above ($T_p > 200$ K).

(3) The fraction of chemisorbed molecules bonded in the η^2-coordination, which requires electron donation from the metal into a π^* orbital of the carbonyl, is suppressed by co-adsorption of oxygen. This has been attributed to competition between the electronegative oxygen and the η^2-carbonyl for electron withdrawal from the metal.[6,7]

We find that 0.005 monolayer of hexafluoroacetone decomposes on Ru(001). There are three desorption states that are distinguishable from the multilayer: α_1 (87 kJ/mol), α_2 (66 kJ/mol), and α_3 (38 kJ/mol). The α_1 state is suppressed by coadsorbed oxygen, while a new state midway between α_2 and α_3 is created. The fact that oxygen induces a *conversion* between chemisorbed states indicates that the oxygen exerts an electronic effect rather than simple site-blocking. All three of these observations, taken together, indicate that the α_1 state represents molecules bonded to the metal via η^2-coordination, whereas the α_3 state represents molecules in the "end-on" (η^1) configuration.

Within the context of this model, a comparison between the chemisorption bond strengths of hydrogenated acetone (ref 7 and this work) and fluorinated acetone (this work) indicates that fluorination weakens the η^1-bond of the chemisorbed carbonyl by 12 kJ/mol, whereas fluorination strengthens the η^2-bond by ca. 20 kJ/mol. The rationale for these trends has been presented in the Introduction. Fluorination also changes the relative distribution of η^1- and η^2-molecules which desorb (cf. Figures 6 and 9), but at this point we cannot say whether that represents a change in the initial populations of adsorbed molecules or a change in the relative rates of competing processes such as desorption and decomposition. In either case, if this model is correct, it is clear that the η^2-bond can form for both the fluorinated and hydrogenated species, i.e., steric hindrance between the CF_3 groups and the metal is not prohibitive in this case. The withdrawal of electron density by the fluorine atoms from oxygen functional group appears to outweigh steric hindrance in determining how the molecule bonds to the Ru surface, in contrast to the observations made by Avery for the Pt(111) surface.[10]

V. Conclusions

Perfluorodiethyl ether bonds to Ru(001) with a lower binding energy than the nonfluorinated compound. This is explained by inductive withdrawal of electron density by the fluorines from the oxygen lone pairs, which weakens the primary chemisorption bond. The CF_2–metal interaction is probably also repulsive because of steric repulsion between the metal and the fluorines. Hexa-

(29) Vedeneyev, V. I.; Gurv'ich, L. V.; Kondrat'yev, V. N.; Medvedev, V. A.; Frankevich, Y. L. *Bond Energies, Ionization Potentials and Electron Affinities*; Edward Arnold Ltd.: London, 1966.

(30) Stacey, M.; Tatlow, J. C.; Sharpe, A. G. *Advances in Fluorine Chemistry*; Butterworths: London, 1961; Vol. 2.

fluoroacetone, with its unsaturated carbonyl group, can form stronger metal-surface bonds, which suggests that some of the molecules bond in an η^2-geometry. Fluorination *decreases* the chemisorption bond strength of the η^1-molecules by about 12 kJ/mol and *increases* that of the η^2-species by about 20 kJ/mol.

Acknowledgment. We thank R. J. Angelici and T. Upton for valuable discussions. This research has been supported by the Director for Energy Research, Office of Basic Energy Sciences. Ames Laboratory is operated for the U.S. Department of Energy by Iowa State University under Contract No. W-7405-ENG-82.

An Inelastic Electron-Tunneling Spectroscopic Investigation of the Reaction of Molybdenum Oxychlorides with a Hydroxylated Aluminum Oxide Surface

G. J. Gajda, R. H. Grubbs, and W. H. Weinberg*

Contribution from the Division of Chemistry and Chemical Engineering, California Institute of Technology, Pasadena, California 91125. *Received January 26, 1987*

Abstract: Molybdenum oxytetrachloride adsorbs on alumina at 22 °C and reacts with the surface hydroxyl groups to form a dimeric oxydichloride–molybdenum complex. This complex desorbs slowly from the surface, as molybdenum dioxodichloride. Heating the surface during oxytetrachloride exposure yields poorly characterized decomposition products and tunnel junctions with very large conductivity changes as a function of bias voltage. Molybdenum dioxodichloride adsorbs on alumina at 22 °C and forms an oligomerized molybdenum trioxide species. This oxide adsorbs water at a background pressure of approximately 1×10^{-7} Torr, and it can be dehydrated by heating under vacuum to 100 °C. Heating the surface during the vapor-phase exposure of molybdenum dioxodichloride, or the molybdenum oxide under vacuum after the exposure, increases the extent of polymerization. Exposure of the oxide to 2 Torr of ethylene at 100 °C or 10^{-1} Torr of acetic acid at 22 °C produces changes in the tunneling spectra, due to increased oligomerization and some decomposition of the adsorbates, but there is no evidence for molecular adsorption or hydrocarbon formation. Exposure of the oxide to 5×10^{-2} Torr of 4-*tert*-butylpyridine at 22 °C causes the complete desorption of the oxide, presumably as the tripyridine complex.

I. Introduction

Inelastic electron-tunneling spectroscopy is a moderate-resolution (full-width at half-maximum below 20 cm^{-1}), high-sensitivity (fractional surface coverages on the order of 10^{-2} monolayer) technique for measuring the vibrational spectra of molecules adsorbed on insulating surfaces. The theory and practice of inelastic electron tunneling have been reviewed extensively,[1-11] as has the more general class of tunneling spectroscopies.[12] The basic requirement of the technique is the formation of a tunnel junction consisting of two conductors separated by a thin insulating barrier. The surface of this insulator is the one upon which adsorption and reaction occurs.

Although many substrates have been used [e.g., Cr,[13] Y,[13] Ho,[14] Er,[14] Al,[15] and Mg[15]], the insulator in most cases has been the metal oxide formed by oxidation in air or a glow discharge. The majority of tunneling spectra have been obtained on the surfaces of Al_2O_3 and MgO.[15] This restriction has led to an investigation of non-oxide insulators and alternative junction geometries (involving movable electrodes) in a search to broaden the range of applications accessible to tunneling spectroscopy.

Non-oxide barriers have been synthesized primarily by employing reagents other than oxygen in the glow discharge treatment of the metal-film electrode. For example, by using CF_4, a barrier similar to AlF_3 is formed,[16] while using $SO_2 + O_2$ produces an AlS_xO_y barrier similar to aluminum disulfate.[17] A second approach has been the evaporation of low-volatile oxides [e.g., SiO[18]] onto the metal substrate. Variations in the junction geometries are represented by the "squeezable" electron-tunnel junctions.[19] In this technique, two separate metal-film electrodes are fabricated and mechanically positioned crosswise, similar to a standard junction geometry but with an air-gap between them. The supported films are then squeezed together by an electromagnet to reduce the gap between the electrodes to approximately 10–20 Å, necessary for electron tunneling to occur. Although no vibrationally inelastic tunneling spectra have yet been reported by this technique, experiments continue.[19] Similarly, theoretical work has appeared, suggesting the measurement of inelastic spectra via scanning tunneling microscopy.[20]

Molybdenum oxide is used widely as a catalyst for oxidation reactions either by itself or in the form of a mixed oxide.[21] We have observed the formation of molybdenum suboxides by decomposition of molybdenum hexacarbonyl on alumina surfaces,[22] but these suboxides were not suitable insulators for tunneling spectroscopy. We have observed also that metal chloride complexes [e.g., $[Rh(CO)_2Cl]_2$[23]] will react with the hydroxylated

(1) Hansma, P. K. *Phys. Rep. C* **1977**, *30*, 146.
(2) Weinberg, W. H. *Annu. Rev. Phys. Chem.* **1978**, *29*, 115.
(3) *Inelastic Electron Tunneling Spectroscopy*; Wolfram, T., Ed.; Springer: Berlin, 1978.
(4) Hansma, P. K.; Kirtley, J. R. *Acc. Chem. Res.* **1978**, *71*, 440.
(5) White, H. W.; Wolfram, T. *Methods Exp. Phys. A* **1980**, *16*, 149.
(6) White, H. W.; Godwin, L. M.; Elliatioglu, R. *J. Adhes.* **1981**, *13*, 177.
(7) Ewert, S. *Appl. Phys. A* **1981**, *26*, 63.
(8) *Tunneling Spectroscopy*; Hansma, P. K., Ed.; Pleunum: New York, 1982.
(9) Weinberg, W. H. *Vib. Spectra Struct.* **1982**, *11*, 1.
(10) Khanna, S. K.; Lambe, J. *Science* **1983**, *220*, 1345.
(11) *Principles of Electron Tunneling Spectroscopy*; Wolf, E. L., Ed.; Oxford: New York, 1985.
(12) Walmsley, D. G.; Tomlin, J. L. *Prog. Surf. Sci.* **1985**, *18*, 247.
(13) Jaklevic, R. C.; Lambe, J. *Phys. Rev. B* **1970**, *2*, 808.
(14) Adane, A. *Solid State Commun.* **1975**, *16*, 1071.
(15) See, for example, the spectra in ref 12.
(16) Gauthier, S.; De Cheveigne, S.; Salace, G.; Klein, J.; Belin, M. *Surf. Sci.* **1985**, *155*, 31.
(17) Suzuki, M.; Mazur, U.; Hipps, K. *Surf. Sci.* **1985**, *161*, 156.
(18) Mazur, U.; Hipps, K. *J. Phys. Chem.* **1981**, *85*, 2244.
(19) Moreland, J.; Alexander, S.; Cox, M.; Sonnenfeld, R.; Hansma, P. K. *Appl. Phys. Lett.* **1983**, *43*, 387.
(20) Binnig, G.; Garcia, N.; Rohrer, H. *Phys. Rev. B* **1985**, *32*, 1336.
(21) See, for example: *Fourth International Conference: The Chemistry and Uses of Molybdenum*; Climax: Ann Arbor, 1982.
(22) Gajda, G. J.; Grubbs, R. H.; Weinberg, W. H. *J. Am. Chem. Soc.* **1987**, *109*, 66.

0002-7863/87/1509-5627$01.50/0